

## Research Article

# Khat (*Catha edulis*) Leaf Extract-Based Zinc Oxide Nanoparticles and Evaluation of Their Antibacterial Activity

Muluken Aklilu <sup>1</sup> and Temesgen Aderaw<sup>2</sup>

<sup>1</sup>Department of Chemistry, Bahir Dar University, Bahir Dar, Ethiopia

<sup>2</sup>Department of Material Science and Engineering, Bahir Dar University, Bahir Dar, Ethiopia

Correspondence should be addressed to Muluken Aklilu; [mulukenak@gmail.com](mailto:mulukenak@gmail.com)

Received 4 June 2022; Revised 19 August 2022; Accepted 1 September 2022; Published 22 September 2022

Academic Editor: Jagpreet Singh

Copyright © 2022 Muluken Aklilu and Temesgen Aderaw. This is an open access article distributed under the Creative Commons Attribution License, which permits unrestricted use, distribution, and reproduction in any medium, provided the original work is properly cited.

In this study, we used khat (*Catha edulis*) leaf extract as a reducing and stabilizing agent for the biosynthesis of zinc oxide nanoparticles (ZnO NPs). The rapid color change of the solution to pale yellow and UV-visible absorption peak at 322 nm confirmed the initial formation of ZnO NPs. FTIR spectrum analysis revealed the contribution of khat leaf extract to the bioreduction of  $Zn^{2+}$  ions to ZnO NPs. The FTIR spectrum for the stretching vibration of ZnO at  $480\text{ cm}^{-1}$  also confirms the formation of ZnO NPs. The XRD spectrum showed the crystallinity and the hexagonal wurtzite structure of ZnO NPs. The size of the synthesized ZnO NPs calculated using the Debye-Scherrer formula was found to be equal to 17 nm. Antibacterial efficacy of green-produced zinc oxide nanoparticles against Gram-positive and Gram-negative microorganisms was tested. It has the greatest inhibition zone (23 mm) against *E. coli*, but the least activity was against *S. pneumoniae* (15 mm).

## 1. Introduction

Green synthesis nanoparticle production through plants, bacteria, fungi, and algae allows for the large-scale production of metal oxide nanoparticles with sizes ranging from 1 to 100 nm [1–4]. Green synthesis is a developing area in the field of chemistry, which aims to design clean products and sustainable processes through decreasing or eliminating the use of toxic reagents [4, 5]. Green synthetic procedures have gained rising popularity as they can develop clean technology that proactively affects the design of nanomaterials and products by decreasing or eliminating toxic wastes from the fabrication of nanoscale materials and provides a benign atmosphere for promoting environmental sustainability [4, 6]. Due to their intrinsic capabilities, green methodologies facilitate the reduction of dissolved metal ions to zero valence state and eventually yield the pertaining nanoparticles [7]. Nanoparticles contain distinct physicochemical, optical, and biological properties that can be customized to fit specific requirements. One of the distinguishing characteristics of nanosized particles is their high surface-to-

volume ratio [8, 9]. Nanoparticles have this property, which allows them to be more reactive than bulk materials because atoms on the surface are more active than those in the bulk [10, 11]. When particles are reduced in size from a micrometer to a nanometer scale, their characteristics such as electrical conductivity, hardness, active surface area, chemical reactivity, and biological activity have all been drastically changed. This is because a large surface area particle has more reaction sites than a small surface area particle [11, 12].

Among the various nanoparticles that have been synthesized so far, zinc oxide nanoparticles (ZnO NPs) have attracted a lot of interest due to their unique physical and chemical characteristics [13, 14]. The attention of the scientific and medical community was drawn to ZnO nanoparticles because of their crucial significance in biomedical and cancer applications. It has many technological applications, because of its exceptional optical and electrical properties, such as thin film transistors [15] and electrochemical sensors [9]. It is also useful in the pharmaceutical and cosmetic industries [16], environmental protection [17], and light-emitting devices and solar cells [18], for rubber industry

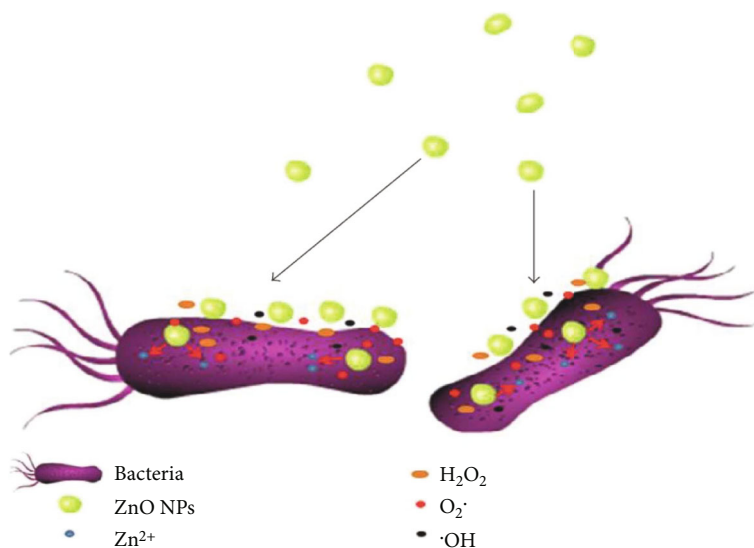


FIGURE 1: Schematic illustration of antibacterial activity of ZnO NPs [19].

[19], improving the efficiency of subgrade soil strength properties [20], heterogeneous and homogeneous catalysts [21], heavy metals absorption [22], and nanomedicine and water purification [7], in food packaging [23] as well as for antibacterial activity [24, 25]. The antibacterial activity may involve the accumulation of ZnO NPs in the outer membrane of bacterial cells and trigger  $\text{Zn}^{2+}$  release, which would cause bacterial cell membrane disintegration, membrane protein damage, and genomic instability, resulting in the death of bacterial cells [19]. As shown in Figure 1, prior reports had suggested that the main antibacterial toxicity mechanisms of ZnO NPs were based on their ability to induce excess reactive oxygen species (ROS) generation, such as superoxide anion, hydroxyl radicals, and hydrogen peroxide production [19, 23]. This puts cells in an oxidative stress state, which causes protein denaturation, affects mitochondrial function and cell metabolic activity, and eventually leads to death [9].

Different physical and chemical processes are now widely used to synthesize metal oxide nanoparticles, allowing one to obtain particles with desired characteristics. Such manufacturing methods are generally excessively costly and involve the use of toxic and hazardous chemicals that cause a variety of environmental risks [6, 26]. As a result, there is a clear need for an alternative, cost-effective, safe, and environmentally friendly technique of nanoparticle synthesis [11, 14, 24, 27].

In recent years, various natural materials such as plant extracts and marine organisms (yeast, bacteria, algae, fungi, etc.) have been exploited to make energy-efficient, low-cost, and nontoxic nanoparticles in the last few decades. They function as a potential biofactory for the reduction and stabilization of the biofabricated nanoparticles owing to a great variety of their secondary metabolite's contents such as polysaccharides, polyphenols, chitosan, alkaloids, fiber, and flavonoids [6, 28]. Furthermore, the presence of a wide array of phytochemicals in their extract may function as a natural stabilizer and/or reducer [29].

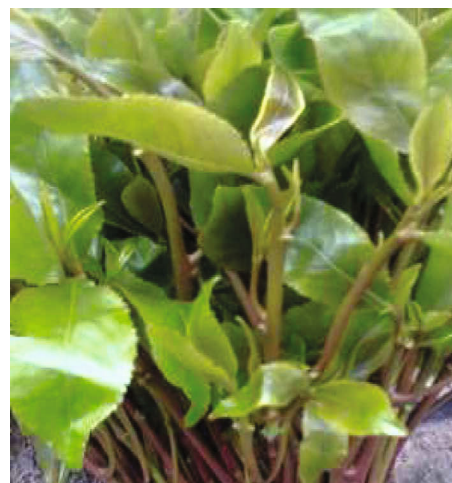


FIGURE 2: Khat (*Catha edulis*) leaf.

According to the previous literatures, ZnO nanoparticles have been synthesized from a variety of plant extracts such as orange fruit peel extract [30], Hibiscus sabdariffa extract [31], Citrus sinensis extract [32], Mangifera indica leaves [33], Andrographis paniculata leaves [34], Parthenium hysterophorus leaf extract [35], tea leaf extract [15], Garcinia mangostana fruit pericarp [36], Aloe vera peel extract [37], etc.

Despite the environmental advantages of using green chemistry-based biological synthesis over traditional methods, there are some unresolved issues such as particle size and shape consistency, reproducibility of the synthesis process, and understanding of the mechanisms involved in producing the nanoparticles via biological entities [38]. Consequently, there is a need for further research to analyze and comprehend the real biological synthesis-dependent processes.

Hence, in this study, khat (*Catha edulis*) leaf extract was used as a reducing and stabilizing agent for the synthesis of zinc oxide nanoparticles. Khat (*Catha edulis*) is an evergreen plant of the family Celastraceae. It is widely cultivated on the

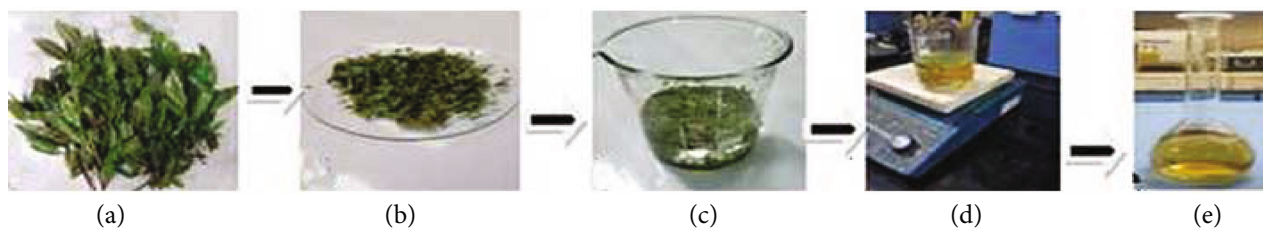


FIGURE 3: The process of khat leaf preparations. (a) Fresh khat leaf, (b) washed khat leaf, (c) small pieces of khat leaf mixed with distilled water, (d) heating of the mixture, and (e) filtrate of khat leaf extract.

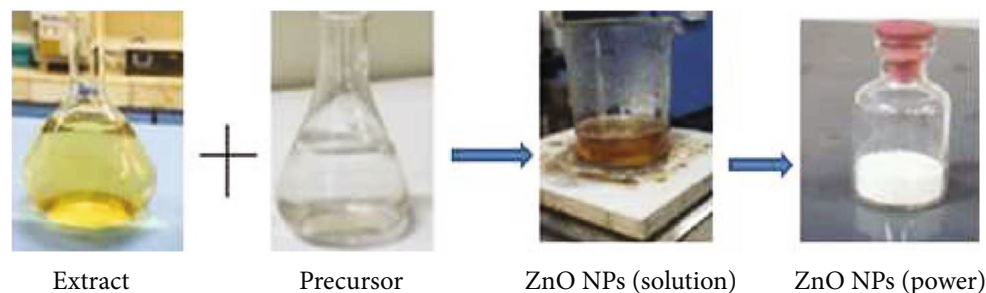


FIGURE 4: Synthesis of zinc oxide nanoparticle preparation.

high and mountain sides of Yemen and Ethiopia (Figure 2) [39, 40]. Khat contains a psychoactive composite belonging to the phenyl propylamine groups of alkaloids called cathinone: a drug that has a stimulant effect on the central nervous system that can be both physically and psychologically addictive when overused [41]. Its young buds and tender leaves are chewed to attain a feeling of great happiness and stimulation [40, 42].

Nowadays, a large number of people in East Africa (Ethiopia, Eritrea, Kenya, Somalia, and Djibouti) and Yemen chew khat leaves because of their pleasurable and stimulating effects [42]. Students have chewed khat in an attempt to improve their mental performance before exams. The leaves have an astringent taste and a characteristic aromatic odor [40]. The taste varies from one type to another due to the different compounds (phytochemicals) present in the leaf. Khat contains more than forty alkaloids, glycosides, tannins, amino acids, vitamins, and minerals [40, 43]. The environmental and climate conditions determine the chemical profile of khat leaves. The presence of phytochemicals and the minor components of khat leaf extract play an important role in the reduction property of khat leaves. The current study focused on the green synthesis of ZnO NPs using khat (*Catha edulis*) leaf extract, and its characterization was investigated along with the evaluation of antibacterial properties for the synthesized ZnO NPs.

## 2. Materials and Methods

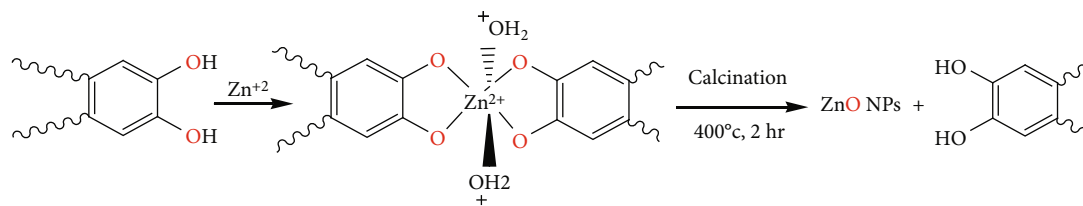
**2.1. Materials and Chemicals.** Khat (*Catha edulis*) leaf was purchased from a local market in Bahir Dar city, Ethiopia. Chemicals such as zinc nitrate hexahydrate, ferric chloride, hydrochloric acid, and sulphuric acid were purchased from Loba Chemie Pvt. Ltd., India. Chemical reagents such as

methanol, gentamycin, chloramphenicol, and potassium bromide from Uvasol, Germany, were also used in the experiment. *Escherichia coli* (Gram-negative), *Salmonella typhi* (Gram-negative), *Staphylococcus aureus* (Gram-positive and Gram-negative bacterial strains), and *Streptococcus pneumoniae* (Gram-positive and Gram-negative bacterial strains) strains purchased from IMTECH, Chandigarh, India. The experiment was conducted with freshly prepared double distilled deionized water, and all of the chemicals used were of analytical grade.

**2.2. Preparation of Khat (*Catha edulis*) Leaf Extract.** Fresh leaves of khat (*Catha edulis*) were washed with tap water followed by double distilled water to remove all contaminants. Thereafter, the leaves were chopped into small pieces and homogenized with a mortar and pestle. The aqueous extract of leaves was made by mixing 5 g of finely chopped leaves with 50 mL of distilled water in a 250 mL glass beaker. The mixture is then heated for 20 minutes at 60°C (Figure 3). After allowing the extract to cool to room temperature, it was filtered through Whatman No. 1 filter paper. The filtrate was put in the refrigerator at 4°C until it was needed for further use.

**2.3. Phytochemical Screening of Khat (*Catha edulis*) Leaf Extracts.** Active constituents in the leaf extract of khat (*Catha edulis*) were detected and identified by performing chemical tests. Phytochemicals such as proteins, tannins, flavonoids, terpenoids, saponins, quinones, and phenols were detected based on standard tests [44–46].

**2.4. Test for Alkaloids.** For this test, a filtrate of khat leaf extract was acidified by adding 1.5% (v/v) of HCl followed by a few drops of Wagner's reagent. The formation of a yellow (orange) precipitate confirmed the presence of alkaloids [44, 46].



SCHEME 1: Possible mechanisms of formation of ZnO NPs by using plant extract [54].



FIGURE 5: Phytochemical analysis of khat (*Catha edulis*) leaf extract for (a) alkaloids, (b) glycosides, (c) flavonoids, (d) steroid, (e) tannins, and (f) phenols.

TABLE 1: Qualitative analysis of phytochemicals in khat (*Catha edulis*) leaf extract.

No.	Phytochemicals	Results	Colors observed
1.	Alkaloid	++	Yellow (orange)
1.	Glycoside	+	Yellow
1.	Flavonoids	++	Yellow
1.	Steroids	++	Reddish brown interface
1.	Tannin	++	Blue-black
1.	Phenols	++	Brown purple

+ = present; ++ = highly present.

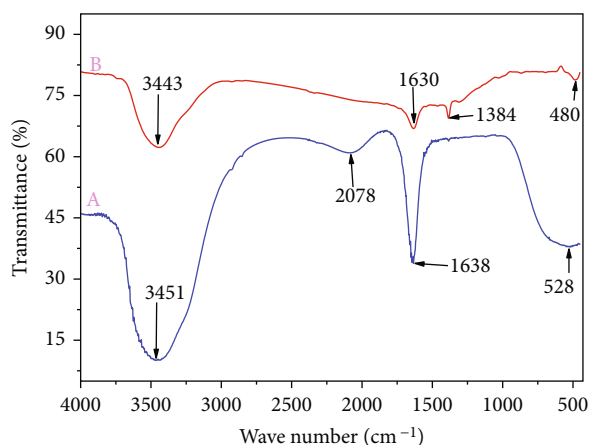


FIGURE 6: FTIR spectra of (a) khat (*Catha edulis*) leaf extract and (b) ZnO NPs.

**2.5. Test for Glycosides.** To test glycosides, a small amount of khat leaf extract was dissolved in 1 mL of water, and 1 mL of aqueous NaOH solution was added to the extract solution.

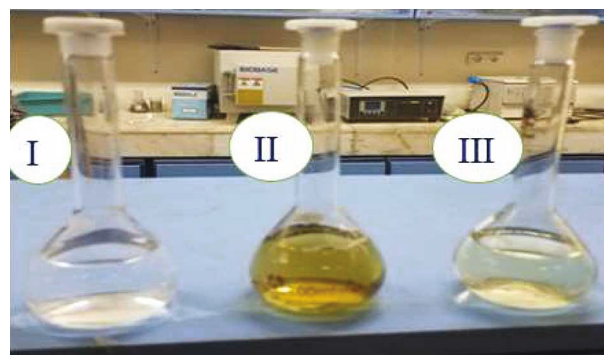


FIGURE 7: Color changes observed before and after the formation of ZnO NPs: (a)  $\text{Zn}(\text{NO}_3)_2 \cdot 6\text{H}_2\text{O}$  solution, (b) leaf extract of khat (*Catha edulis*), and (c) ZnO NPs.

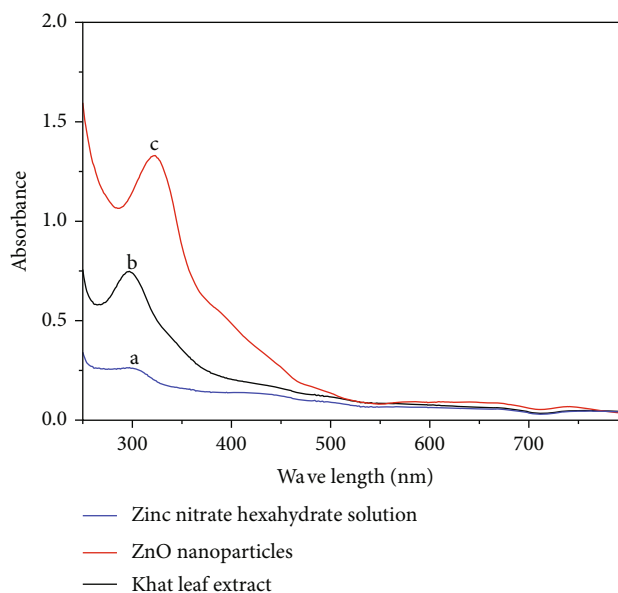


FIGURE 8: UV-visible spectra of (a) precursor, (b) khat leaf extract, and (c) ZnO NPs.

The formation of a yellow color confirmed the presence of glycosides [44].

**2.6. Test for Flavonoids.** For the flavonoids test, 5 mL of dilute ammonia was added to 3 mL of aqueous filtrate of khat leaf extract. This was followed by the addition of 1.5 mL of concentrated sulphuric acid ( $\text{H}_2\text{SO}_4$ ). The formation of a yellow color confirmed the presence of flavonoids [46].

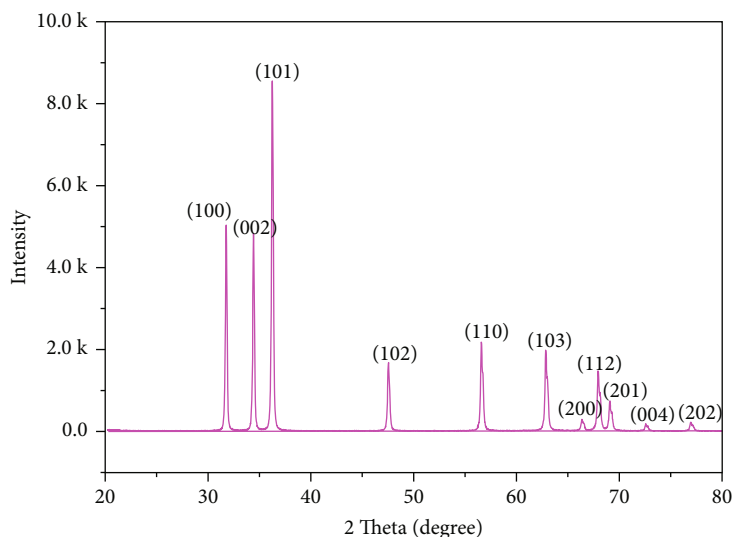


FIGURE 9: X-ray diffraction patterns of ZnO nanoparticles.

**2.7. Test for Steroids.** For the steroids test, 2 mL of khat extract was mixed with 2 mL of chloroform, and 1 mL of concentrated  $H_2SO_4$  was added carefully to the mixture. The appearance of a reddish brown color interface indicated the presence of steroids [45].

**2.8. Test for Tannins.** For the tannins test, 3 mL of khat leaf extract was placed in the test tube, and then, 2 mL of 5% ferric chloride solution was added. The formation of a brownish green or blue-black color confirmed the presence of tannins [44, 46].

**2.9. Test for Phenols.** For the phenols test, 1 mL of khat leaf extract and 2 mL of distilled water followed by a few drops of 5% ferric chloride were added. The formation of brown-purple color confirmed the presence of phenols [44].

**2.10. Synthesis of Zinc Oxide Nanoparticles.** To synthesize zinc oxide nanoparticles, a 2 mL aqueous solution of 3% (*w/v*) khat (*Catha edulis*) leaf extract was mixed with 5 mL of a 1 mM aqueous  $Zn(NO_3)_2 \cdot 6H_2O$  solution. We heated the solution for 10 minutes at a temperature of  $60^\circ C$  using a magnetic stirrer (Figure 4). The solution color changes to yellow due to the formation of a  $Zn^{2+}$  complex with the phytochemical components of the khat leaf (Scheme 1). The resulting solution was placed in a Petri dish and heated in the oven at  $400^\circ C$  for two hours. After calcination, a white powder of zinc oxide was packaged and kept in the sample container for the next characterization.

**2.11. Characterization of Zinc Oxide Nanoparticles.** Visual inspection, UV-visible absorption spectroscopy, X-ray diffraction spectroscopy, and FTIR spectroscopic analyses were used to evaluate ZnO NPs produced using khat leaf extract. Every color change for each phase of the nanoparticle produced was carefully observed. The color changes were blended and examined before and after the khat (*Catha edulis*) leaf extract and the precursor were mixed. The UV-visible absorption spectral analysis of the produced ZnO NPs was

performed using an Agilent Cary 60 UV-vis spectrophotometer. The samples of the combination were closely monitored to ensure that the bioreduction of  $Zn^{2+}$  ions was complete and then scanned in the UV-visible spectrum with wavelengths ranging from 200 to 700 nm. A drop of the extract was combined with KBr powder to prepare a paste for FTIR spectroscopic measurement. The paste was then scanned with an 8 nm resolution FTIR spectroscopy in the wave number range of 400 to  $4000\text{ cm}^{-1}$ . The crystalline nature of the zinc oxide nanoparticle was measured using X-ray diffraction (XRD, PANalytical X'Pert PRO) with Cu K radiation at a voltage of 40 kV and a current of 30 mA. The average size of ZnO NPs was calculated using the Debye-Scherrer equation.

**2.12. Antibacterial Activity of ZnO NPs Using Disc Diffusion Methods.** The disc diffusion method was used to test the antibacterial activity of ZnO NPs against human pathogens *Escherichia coli* (Gram-negative), *Salmonella typhi* (Gram-negative), *Staphylococcus aureus* (Gram-positive), and *Streptococcus pneumoniae* (Gram-positive). Before being placed on the agar, the discs were soaked using sterile forceps in double distilled water as a negative control, ZnO nanoparticles colloidal solution, plant leaves extract, and 2 mM zinc nitrate solution. As a positive control, gentamicin and chloramphenicol were inserted in the center of the plates. Each disc was gently pressed down with sterile forceps to ensure precise contact with the agar surface. The agar plates were then incubated for 24 hours at  $37^\circ C$ . The inhibition zones that resulted were measured, and they were expected to be uniformly round with a confluent lawn of development. A digital electronic caliper was used to measure the sizes of zones of full inhibition. Antibiotics gentamicin and chloramphenicol were used as positive control.

### 3. Results and Discussion

**3.1. Phytochemical Analysis of Khat (*Catha edulis*) Leaf Extract.** Phytochemicals are plant-derived bioactive compounds. They are classified as secondary metabolites since

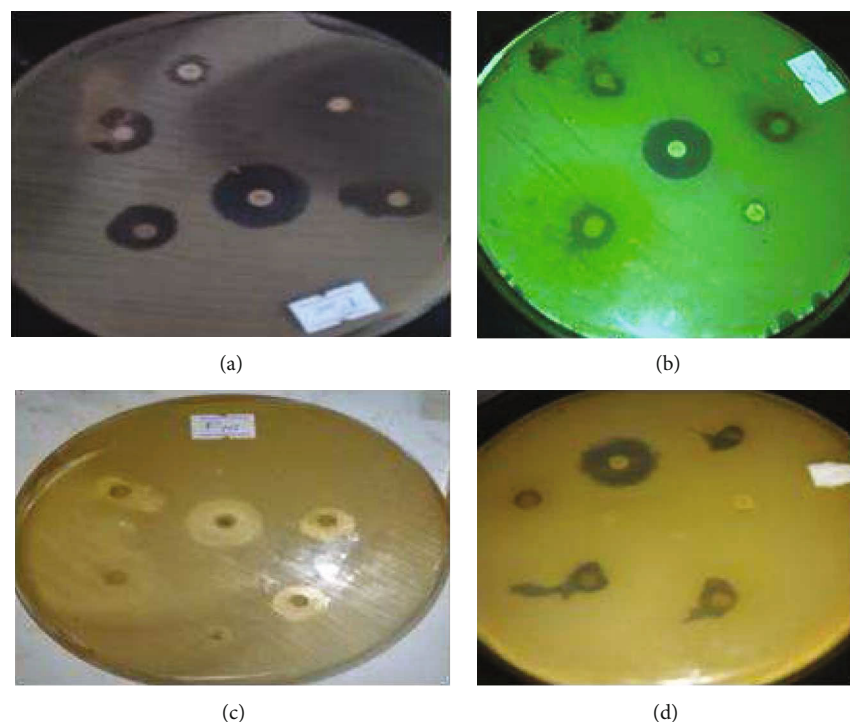


FIGURE 10: Antibacterial image of ZnO nanoparticles: (a) *E. coli*, (b) *S. typhi*, (c) *S. aureus*, and (d) *S. pneumoniae*.

the plants that make them may not require them. All parts of the plant, including the leaves, stem, root, flower, fruits, and seeds, produce them naturally [47]. Alkaloids, glycosides, flavonoids, steroids, tannins, and phenols were identified in the preliminary phytochemical screening of khat (*Catha edulis*) leaf extract. Standard procedures were used to identify these phytochemical constituents based on color changes (Figure 5) [48, 49]. Table 1 shows the results of a qualitative phytochemical investigation of khat (*Catha edulis*) leaf extract. From the table, it is observed that khat (*Catha edulis*) leaf extract showed the presence of phytoconstituents.

**3.2. The FTIR Spectra Analysis.** Photochemical of khat (*Catha edulis*) leaf extract that are responsible for reducing, capping, and stabilization of ZnO NPs was determined using FTIR spectroscopic measurements. The FTIR spectrum of plant extracts and manufactured ZnO NPs is shown in Figures 6(a) and 6(b), respectively. The presence of a strong, broadband spectrum (Figure 6(a)) at  $3451\text{ cm}^{-1}$  in khat (*Catha edulis*) leaf extract can be attributed to hydrogen linked O-H stretching vibrations of phenol, alcohol, carboxylic groups, and other compounds [50, 51]. At  $3443\text{ cm}^{-1}$ , a broad absorption band for the synthesized ZnO NPs was also observed (Figure 6(b)). Alcohols, phenolics, carboxylic groups, and other OH stretching vibrations are associated with the spectrum [4, 10, 15]. When compared to the spectra of khat (*Catha edulis*) leaf extract, the intensity of this spectrum is reduced and its location is shifted [36, 52]. The reason for the reduction of the spectra is due to the fact that the phytochemicals such as alcohols, flavones, and carboxylic groups are involved for the reduction of  $\text{Zn}^{2+}$  to ZnO nanoparticles [10, 36]. A strong absorption spectra for khat leaf extract (Figure 6(a)) was observed at  $1638\text{ cm}^{-1}$ , which may

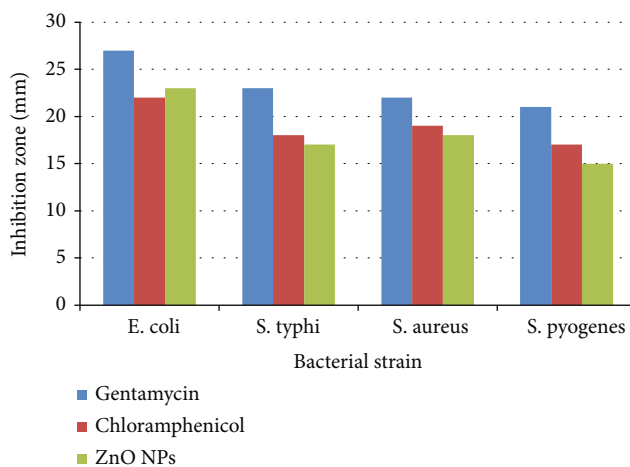


FIGURE 11: Antibacterial activity of ZnO nanoparticles against bacterial strains.

be attributed to C=O bands and the N-H group of proteins and enzymes [13, 23, 51]. The spectra of C=O bands and the N-H group of proteins and enzymes for the biosynthesized ZnO NPs shifts to  $1630\text{ cm}^{-1}$ , and the intensity is significantly decreased (Figure 6(b)). The decrease in intensity is mainly due to the redox reaction of C=O containing organic compounds with zinc ions which converts to the OH group [4, 26, 50]. This is also another confirmation test for the involvement of phytochemicals in the reduction process. The stretching vibration of ZnO has an absorption spectrum of  $480\text{ cm}^{-1}$ , confirming the production of zinc oxide nanoparticles [10, 35, 53]. The presence of N-H and O-H bonds in the FTIR spectrum revealed that proteins

TABLE 2: Zone of inhibition of ZnO NPs against different human pathogenic bacterial strains.

Reagent	E. coli inhibition zone (mm)	S. typhi inhibition zone (mm)	S. aureus inhibition zone (mm)	S. pneumoniae inhibition zone (mm)
Gentamycin	27	23	22	21
Chloramphenicol	22	18	18	17
[3]	13	—	16	10
[51]	19.8	—	10.7	—
ZnO NPs	23	17	17	15

and phenolic and flavonoid compounds are responsible for the bioreduction and stabilization process of ZnO NPs synthesis [51]. The stabilization of the synthesized ZnO NPs may be due to the coordination of ZnO NPs with  $-OH$  and  $C=O$  groups [15].

The mechanism of ZnO NPs synthesis is that the plant extracts act ligation and the aromatic hydroxyl group present in polyphenolic ellagic acid ligate with  $Zn^{2+}$  ions to form zinc-ellagate complex (Scheme 1). Calcination of the complex for 2 hours at a temperature of  $400^\circ C$  results in the formation of white powder (ZnO NPs) [54].

**3.3. Visual Observation.** Confirmation of ZnO NPs formation in colloidal solution was easily noticeable due to a change in the color of the colloidal solution after the addition of  $Zn(NO_3)_2 \cdot 6H_2O$  to the leaf extract. The colorless  $Zn(NO_3)_2 \cdot 6H_2O$  solution started changing its color to pale yellow as soon as the leaf extract of khat (*Catha edulis*) was added (Figure 7). This color change to pale yellow confirms the formation of ZnO NPs, which is in agreement with the previous work [4, 16].

**3.4. UV-Visible Spectra Analysis.** The characterization of ZnO NPs by visual examination was further confirmed by UV-visible spectroscopic analysis. The UV-vis spectra of ZnO NPs showed a distinct maximum absorbance peak at 322 nm (Figure 8). The spectra showed no additional peaks, indicating that the produced products are pure ZnO NPs. The spectra recorded, implied that most rapid bioreduction was achieved using khat (*Catha edulis*) leaf extract. This result definitely agrees with the range of  $\lambda_{max}$  values of the ZnO NPs reported by the previous researchers [51]. Furthermore, it has been found that the peak positions of UV-visible spectra are related to nanoparticle size, with blue shifting as nanoparticle crystal size decreases [3]. The UV-vis spectra in this investigation indicated a blue shift in wavelength, which can be interpreted as a sign of ZnO NPs with tiny particle sizes. As a result, visual inspection and UV-vis spectrum values are used to confirm the synthesis of ZnO NPs.

The possible reaction mechanism of ZnO NP formation is the reduction of zinc ions ( $Zn^{2+}$ ) using phytochemicals (flavonoids, terpenoids, and tannins) to zero-valent Zn atoms. These zero-valent Zn atoms start the nucleation process and are involved in converting the remaining  $Zn^{2+}$  to ZnO, which leads to cluster formation [51].

**3.5. XRD Analysis.** The XRD spectrum of the synthesized ZnO nanoparticles offers information on structural identification and crystalline size determination. XRD spectra of ZnO nanoparticles synthesized using zinc acetate hexahydrate and khat (*Catha edulis*) leaf extract are shown in Figure 9. Cu  $K\alpha$  radiation ( $k = 0.15406$  nm) and  $2\theta$  ranges from  $10^\circ$  to  $80^\circ$  were used to measure the diffraction peaks. The diffraction peaks found at  $2\theta$  values are  $31.78^\circ$ ,  $34.44^\circ$ ,  $36.27^\circ$ ,  $47.56^\circ$ ,  $56.61^\circ$ ,  $62.87^\circ$ ,  $66.39^\circ$ ,  $67.96^\circ$ ,  $69.10^\circ$ ,  $72.64^\circ$ , and  $77.03^\circ$ , respectively. The peaks correspond to the lattice planes of (100), (002), (101), (102), (110), (103), (200), (112), (201), (004), and (202). The diffraction peaks were assigned using JCPDS file card No. 0361451 [4, 23]. The characteristic peaks obtained for ZnO NPs are in good agreement with the previous experimental findings. From the spectra, it is possible to conclude that the structure of ZnO NPs is hexagonal wurtzite structure [10, 12, 50]. The crystallite size ( $D$ ) of ZnO NPs was calculated from the full width at half maximum of XRD spectra by using the Debye-Scherrer equation:

$$D = \frac{K\lambda}{\beta \cos \theta}, \quad (1)$$

where  $D$  is the crystallite size,  $\lambda = 0.15406$  nm, which is the wavelength of the X-ray for Cu target  $K\alpha$  radiation;  $\beta$  is the peak width at half maximum of an XRD,  $K = 0.89$ , which is the Scherrer's constant; and  $\theta$  is the Bragg diffraction angle.

The full width at half maximum was measured using Gaussian curve for the highest peak. Thus, the crystalline size of the synthesized ZnO NPs calculated using Debye-Scherrer formula was found to be equal to 17 nm.

**3.6. Antibacterial Activity.** Using the agar well-diffusion method, the antibacterial activity of ZnO NPs produced from khat leaf extract was tested against Gram-negative and Gram-positive pathogenic bacteria. The pathogenic bacteria used for the test were *Escherichia coli*, *Salmonella typhi*, *Staphylococcus aureus*, and *Streptococcus pneumoniae*. Antibiotics gentamycin and chloramphenicol were used as positive control. The antibacterial activity of ZnO NPs was determined on the basis of zone of inhibition (mm). Figure 10 depicts a graph of ZnO nanoparticle protection levels against several bacterial strains. *E. coli* was used to determine the maximum zone of inhibition (23 nm). The zone of inhibition for *Staphylococcus aureus* and *Salmonella*

typhi was moderate; however, the zone of inhibition for *Streptococcus pneumoniae* was modest (Figure 11).

The structure and chemical makeup of the microorganisms' cell membranes may play a role in their antibacterial activity difference [50]. From the table, it is observed that ZnO NPs synthesized in this study are good candidates for their usage in antibacterial drugs, but the principal antibacterial mechanism of metal and metal oxide nanoparticles remains relatively unclear. It is found that nanoparticles functionalized with biomolecule can significantly enhance antimicrobial activity [6]. Thus, it is vital to investigate the mechanisms of ZnO NP bactericidal activity before they may be employed as an antibacterial material. The interaction of ZnO NPs with the outer surface of the plasma membrane is one mechanism of antibacterial activity. This contact alters the permeability of the plasma membrane by disrupting its structure. The disruption of membrane structure and consequent accumulation of ZnO NPs in the cytoplasm interferes with the basic cell development processes [23].

As shown in Table 2, the antibacterial activity efficiency of the synthesized ZnO NPs is better than the literature values.

#### 4. Conclusions

In this study, ZnO NP was effectively produced via a green synthetic process with the help of khat (*Catha edulis*) leaf extract as a reducing, stabilizing, and capping agent. This synthetic approach is easy to use, inexpensive, and safe for the environment. The synthesized zinc oxide nanoparticles were characterized using visual observation (color change), UV-vis absorption spectroscopy, XRD, and FTIR spectroscopy. UV-visible absorption spectrum showed a distinct peak around 322 nm, which is specific for ZnO NPs. From the FTIR spectroscopic result, it is observed that khat leaf extract contains various phytochemicals. The spectrum at  $480\text{ cm}^{-1}$ , which was not present in the pure extract, is thought to be the most important confirmation of ZnO NP formation. Our results confirm the potential of khat leaf extract for the synthesis of ZnO NPs in a fast and ecofriendly way. Powder X-ray diffraction examination confirmed the crystalline nature and hexagonal wurtzite structure of the synthesized ZnO NPs. The crystalline size of ZnO NPs synthesized by zinc acetate hexahydrate and khat leaf extract was found to be 17 nm. ZnO NPs synthesized using the above green method have better antibacterial activity against Gram-negative bacteria than Gram-positive bacteria. It has a maximum inhibition zone of 23 mm for *Escherichia coli* and a minimum inhibition zone of 15 mm for *Streptococcus pneumoniae*.

#### Data Availability

All the available data are presented in the manuscript.

#### Conflicts of Interest

The authors declare that there are no conflicts of interest for this work.

#### References

- [1] J. Suresh, G. Pradheesh, V. Alexramani, M. Sundrarajan, and S. I. Hong, "Green synthesis and characterization of zinc oxide nanoparticle using insulin plant (*Costus pictus* D. Don) and investigation of its antimicrobial as well as anticancer activities," *Advances in Natural Sciences: Nanoscience and Nanotechnology*, vol. 9, no. 1, article 015008, 2018.
- [2] S. Abe, J. L. Tesfaye, R. Shanmugam et al., "Green synthesis and characterizations of zinc oxide (ZnO) nanoparticles using aqueous leaf extracts of coffee (*Coffea arabica*) and its application in environmental toxicity reduction," *Journal of Nanomaterials*, vol. 2021, Article ID 3413350, 6 pages, 2021.
- [3] M. G. Demissie, F. K. Sabir, G. D. Edossa, and B. A. Gonfa, "Synthesis of zinc oxide nanoparticles using leaf extract of *Lippia adoensis* (Koseret) and evaluation of its antibacterial activity," *Journal of Chemistry*, vol. 2020, Article ID 7459042, 9 pages, 2020.
- [4] T. Khalaf, F. Buazar, and K. Ghanemi, "Phycosynthesis and enhanced photocatalytic activity of zinc oxide nanoparticles toward organosulfur pollutants," *Scientific Reports*, vol. 9, no. 6886, pp. 1–10, 2019.
- [5] M. Sepahvand, F. Buazar, and M. H. Sayahi, "Novel marine-based gold nanocatalyst in solvent-free synthesis of polyhydroquinoline derivatives: green and sustainable protocol," *Applied Organometallic Chemistry*, vol. 34, no. 12, pp. 1–11, 2020.
- [6] N. H. Rezazadeh, F. Buazar, and S. Matroodi, "Synergistic effects of combinatorial chitosan and polyphenol biomolecules on enhanced antibacterial activity of biofunctionalized silver nanoparticles," *Scientific Reports*, vol. 10, no. 1, pp. 1–13, 2020.
- [7] S. Safat, F. Buazar, S. Albukhaty, and S. Matroodi, "Enhanced sunlight photocatalytic activity and biosafety of marine-driven synthesized cerium oxide nanoparticles," *Scientific Reports*, vol. 11, no. 1, pp. 1–11, 2021.
- [8] R. Saemi, E. Taghavi, H. Jafarizadeh-Malmiri, and N. Anarjan, "Fabrication of green ZnO nanoparticles using walnut leaf extract to develop an antibacterial film based on polyethylene-starch-ZnO NPs," *Green Processing and Synthesis*, vol. 10, no. 1, pp. 112–124, 2021.
- [9] J. Xu, Y. Huang, S. Zhu, N. Abbas, X. Jing, and L. Zhang, "A review of the green synthesis of ZnO nanoparticles using plant extracts and their prospects for application in antibacterial textiles," *Journal of Engineered Fibers and Fabrics*, vol. 16, article 155892502110462, 2021.
- [10] S. Narendhran and R. Sivaraj, "Biogenic ZnO nanoparticles synthesized using *L. aculeata* leaf extract and their antifungal activity against plant fungal pathogens," *Bulletin of Materials Science*, vol. 39, no. 1, pp. 1–5, 2016.
- [11] E. R. Carmona, N. Benito, T. Plaza, and G. Recio-Sánchez, "Green synthesis of silver nanoparticles by using leaf extracts from the endemic *Buddleja globosa*," *Green Chemistry Letters and Reviews*, vol. 10, no. 4, pp. 250–256, 2017.
- [12] A. A. Barzinjy and H. H. Azeez, "Green synthesis and characterization of zinc oxide nanoparticles using *Eucalyptus globulus* Labill. leaf extract and zinc nitrate hexahydrate salt," *SN Applied Sciences*, vol. 2, no. 5, pp. 1–14, 2020.
- [13] M. S. Geetha, H. Nagabhushana, and H. N. Shivananjaiiah, "Green mediated synthesis and characterization of ZnO nanoparticles using *Euphorbia jatropha* latex as reducing agent," *Journal of Science: Advanced Materials and Devices*, vol. 1, no. 3, pp. 301–310, 2016.



- [14] S. Faisal, H. Jan, S. A. Shah et al., "Green synthesis of zinc oxide (ZnO) nanoparticles using aqueous fruit extracts of myristica-fragrans: their characterizations and biological and environmental applications," *ACS Omega*, vol. 6, pp. 9707–9722, 2021.
- [15] P. Sutradhar and M. Saha, "Synthesis of zinc oxide nanoparticles using tea leaf extract and its application for solar cell," *Bulletin of Materials Science*, vol. 38, no. 3, pp. 1–5, 2015.
- [16] M. Manokari, R. Latha, S. Priyadarshini, R. M. Cokul, P. Beniwal, and M. S. Shekhawat, "Green synthesis of zinc oxide nanoparticles from aqueous extracts of Sesamumindicum L. and their characterization," *World News of Natural Sciences*, vol. 23, pp. 200–210, 2019.
- [17] S. Pal, S. Mondal, J. Maity, and R. Mukherjee, "Synthesis and characterization of ZnO nanoparticles using Moringa oleifera leaf extract: investigation of photocatalytic and antibacterial activity," *International Journal of Nanoscience and Nanotechnology*, vol. 14, no. 2, pp. 111–119, 2018.
- [18] S. Azizi, R. Mohamad, and M. M. Shahri, "Green microwave-assisted combustion synthesis of zinc oxide nanoparticles with Citrullus colocynthis (L.) Schrad: characterization and biomedical applications," *Molecules*, vol. 22, no. 2, pp. 301–313, 2017.
- [19] J. Jiang, J. Pi, and J. Cai, "The advancing of zinc oxide nanoparticles for biomedical applications," *Bioinorganic Chemistry and Applications*, vol. 2018, Article ID 1062562, 18 pages, 2018.
- [20] F. Buazar, "Impact of biocompatible nanosilica on green stabilization of Subgrade soil," *Scientific Reports*, vol. 9, no. 1, pp. 1–9, 2019.
- [21] J. Moavi, F. Buazar, and M. H. Sayahi, "Algal magnetic nickel oxidenanocatalyst in accelerated synthesis of pyridopyrimidinederivatives," *Scientific Reports*, vol. 11, no. 1, pp. 1–14, 2021.
- [22] K. Hardani, F. Buazar, K. Ghanemi et al., "Removal of toxic mercury (II) from water via Fe<sub>3</sub>O<sub>4</sub>/hydroxyapatite nanoadsorbent: an efficient, economic and rapid approach," *AASCIT Journal of Nanoscience*, vol. 11, no. 6296, pp. 1–14, 2021.
- [23] P. Jamdagni, P. Khatri, and J. S. Rana, "Green synthesis of zinc oxide nanoparticles using flower extract of Nyctanthes arbor-tristis and their antifungal activity," *Journal of King Saud University–Science*, vol. 10, no. 2, pp. 1–8, 2016.
- [24] N. K. Rajendran, B. P. George, N. N. Houreld, and H. Abrahamse, "Synthesis of zinc oxide nanoparticles using Rubusfairholmianus root extract and their activity against pathogenic bacteria," *Molecules*, vol. 26, no. 3029, pp. 1–11, 2021.
- [25] A. Azam, A. S. Ahmed, M. Oves, M. S. Khan, S. S. Habib, and A. Memic, "Antimicrobial activity of metal oxide nanoparticles against Gram-positive and Gram-negative bacteria: a comparative study," *International Journal of Nanomedicine*, vol. 7, pp. 6003–6009, 2012.
- [26] H. Koopi and F. Buazar, "A novel one-pot biosynthesis of pure alpha aluminum oxide nanoparticles using the macroalgae Sargassum ilicifolium: a green marine approach," *Ceramics International*, vol. 1, no. 1, pp. 11–18, 2015.
- [27] S. Yedurkar, C. Maurya, and P. Mahanwar, "Biosynthesis of zinc oxide nanoparticles using Ixora coccinea leaf extract—a green approach," *Open Journal of Synthesis Theory and Applications*, vol. 5, no. 1, pp. 1–14, 2016.
- [28] S. Fakhari, M. Jamzad, and H. K. Fard, "Green synthesis of zinc oxide nanoparticles: a comparison," *Green Chemistry Letters and Reviews*, vol. 12, no. 1, pp. 19–24, 2019.
- [29] Y. A. Selim, M. A. Azb, I. Ragab, and M. H. M. A. El-Azim, "Green synthesis of zinc oxide nanoparticles using aqueous extract of Deverra tortuosa and their cytotoxic activities," *Scientific Reports*, vol. 10, no. 3445, pp. 1–9, 2020.
- [30] T. U. D. Thi, T. T. Nguyen, Y. D. Thi, K. H. T. Thi, B. T. Phanbc, and K. N. Pham, "Green synthesis of ZnO nanoparticles using orange fruit peel extract for antibacterial activities," *RSC Advances*, vol. 10, no. 23899, pp. 1–9, 2020.
- [31] C. A. Soto-Roblesa, P. A. Luquea, C. M. Gómez-Gutiérrez et al., "Study on the effect of the concentration of Hibiscus sabdariffa extract on the green synthesis of ZnO nanoparticles," *Results in Physics*, vol. 15, article 102807, Article ID 10.1016/j.rinp.2019.102807, 2019.
- [32] P. A. Luque, C. A. Soto-Robles, O. Nava et al., "Green synthesis of zinc oxide nanoparticles using Citrus sinensis extract," *Journal of Materials Science: Materials in Electronics*, vol. 29, no. 12, pp. 9764–9770, 2018.
- [33] B. S. A. Narayana, K. Pandey, N. Azmi, M. Tejashwini, U. Shrestha, and S. V. Lokesh, "Synthesis and characterization of zinc oxide (zno) nanoparticles using mango (mangifera-indica) leaves," *International Journal of Research and Analytical Reviews*, vol. 5, no. 3, pp. 432–439, 2018.
- [34] S. Kavitha, M. Dhamodaran, R. Prasad, and M. Ganesan, "Synthesis and characterisation of zinc oxide nanoparticles using terpenoid fractions of Andrographis paniculata leaves," *International Nano Letters*, vol. 7, no. 2, pp. 141–147, 2017.
- [35] A. Datta, C. Patra, H. Bharadwaj, S. Kaur, N. Dimri, and R. Khajuria, "Green synthesis of zinc oxide nanoparticles using Parthenium hysterophorus leaf extract and evaluation of their antibacterial properties," *Journal of Biotechnology and Biomaterials*, vol. 7, no. 3, pp. 1–5, 2017.
- [36] M. Aminuzzaman, L. P. Ying, W. Goh, and A. Watanabe, "Green synthesis of zinc oxide nanoparticles using aqueous extract of Garcinia mangostana fruit pericarp and their photocatalytic activity," *Bulletin of Materials Science*, vol. 41, no. 50, pp. 1–10, 2018.
- [37] A. Chaudhary, N. Kumar, R. Kumar, and R. K. Salar, "Antimicrobial activity of zinc oxide nanoparticles synthesized from Aloe vera peel extract," *SN Applied Sciences*, vol. 1, no. 1, pp. 1–9, 2019.
- [38] H. Chopra, S. Bibi, I. Singh et al., "Green metallic nanoparticles: biosynthesis to applications," *Frontiers in Bioengineering and Biotechnology*, vol. 10, pp. 1–29, 2022.
- [39] A. Al-Alimi, T. Taiyeb-Ali, N. Jaafar, and N. N. Al-hebshi, "Qat chewing and periodontal pathogens in health and disease: further evidence for a prebiotic-like effect," *BioMed Research International*, vol. 2015, Article ID 291305, 7 pages, 2015.
- [40] N. T. Wabe, "Psychopharmacological aspects of Catha edulis (khat) and consequences of long term use: a review," *Journal of Mood Disorders*, vol. 1, no. 4, pp. 187–194, 2010.
- [41] Z. T. Tadesse, *Geographic variation and factors associated with khat chewing among adult males 15-59 years in Ethiopia, EDHS 2016. generalized estimating equation approach*, Research Square, 2019.
- [42] M. A. Zahran, A. Khedr, A. Dahmash, and Y. A. El-Ameir, "Qat farms in Yemen: ecology, dangerous impacts and future promise," *Egyptian Journal of Basic and Applied Sciences*, vol. 1, no. 1, pp. 107–114, 2014.
- [43] R. H. Al-Ashwal, M. A. Al-Maqtari, K. M. Najji, N. A. Alwsabai, and S. M. Al Hazmy, "Potential health effects of daily khat leaves chewing: study on the biochemical blood constituents changes among adults in Sana'a city, Yemen," *International*

- Journal of Biochemistry and Biotechnology*, vol. 2, no. 6, pp. 1–5, 2013.
- [44] U. S. M. Rao, M. Abdurrazak, and K. S. Mohd, “HYTOCHEMICAL screening, total flavonoid and phenolic content assays of various solvent extracts of tepal of *Musa paradisiaca*,” *Malaysian Journal of Analytical Sciences*, vol. 20, no. 5, pp. 1181–1190, 2016.
- [45] R. Gul, S. U. Jan, S. Faridullah, S. Sherani, and N. Jahan, “Preliminary phytochemical screening, quantitative analysis of alkaloids, and antioxidant activity of crude plant extracts from *Ephedra intermedia* Indigenous to Balochistan,” *The Scientific World Journal*, vol. 2017, Article ID 5873648, 7 pages, 2017.
- [46] S. Sankhalkar and V. Vernekar, “Quantitative and qualitative analysis of phenolic and flavonoid content in *Moringa oleifera* Lam and *Ocimum tenuiflorum* L.,” *Pharmacognosy Research*, vol. 8, no. 1, pp. 16–21, 2016.
- [47] P. Obazelu, A. Aruomaren, and E. E. Ugboaja, “Phytochemical analysis, nutrients and mineral composition of *Combretum platypterum* aqueous leaf extract,” *Journal of Applied Sciences and Environmental Management*, vol. 25, no. 9, pp. 1625–1630, 2021.
- [48] Z. Abdisa and F. Kenea, “Phytochemical screening, antibacterial and antioxidant activity studies on the crude root extract of *Clematis hirsute*,” *Cogent Chemistry*, vol. 6, pp. 1–10, 2021.
- [49] Y. Hassan and M. I. Barde, “Phytochemical screening and antioxidant potential of selected Nigerian *Kahraman*,” *International Annals of Science*, vol. 8, no. 1, pp. 12–16, 2020.
- [50] S. Azizi, R. Mohamad, and M. M. Shahri, “Green microwave-assisted combustion synthesis of zinc oxide nanoparticles with *Citrullus colocynthis* (L.) Schrad: characterization and biomedical applications,” *Molecules*, vol. 22, no. 301, pp. 1–13, 2017.
- [51] G. Sharmila, C. Muthukumaran, K. Sandiya et al., “Biosynthesis, characterization, and antibacterial activity of zinc oxide nanoparticles derived from *Bauhinia tomentosa* leaf extract,” *Journal of Nanostructure in Chemistry*, vol. 8, no. 3, pp. 293–299, 2018.
- [52] S. Umavathi, M. Ramya, C. Padmapriya, and K. Gopinath, “Green synthesis of zinc oxide nanoparticle using *Justicia procumbens* leaf extract and their application as an antimicrobial agent,” *Journal of Biologically Active Products from Nature*, vol. 10, no. 2, pp. 153–164, 2020.
- [53] F. Buazar, M. Bavi, F. Kroushawi, M. Halvani, A. Khaledi-Nasab, and S. A. Hossieni, “Potato extract as reducing agent and stabiliser in a facile green one-step synthesis of ZnO nanoparticles,” *Journal of Experimental Nanoscience*, vol. 11, no. 3, pp. 175–184, 2016.
- [54] O. Kahraman, R. Binzet, E. Turunc, A. Dogen, and H. Arslan, “Synthesis, characterization, antimicrobial and electrochemical activities of zinc oxide nanoparticles obtained from *Sarcopoterium spinosum* (L.) spach leaf extract,” *Materials Research Express*, vol. 5, no. 11, pp. 1–15, 2018.